DOI: 10.1002/((please add manuscript number))

Article type: Communication

Anomalous Diffusion-Assisted Brightness in White Cellulose Nanofibril Membranes

Matti S. Toivonen[+], Olimpia D. Onelli[+], Gianni Jacucci, Ville Lovikka, Orlando J. Rojas, Olli Ikkala, and Silvia Vignolini**

M. S. Toivonen, Prof. O. J. Rojas, Prof. O. Ikkala
Department of Applied Physics, Aalto University School of Science, P.O. Box 15100, FI-00076, Espoo, Finland.
Email: Olli.ikkala@aalto.fi

V. Lovikka, Prof. O. J. Rojas, Prof. O. Ikkala
Department of Bioproducts and Biosystems, Aalto University School of Chemical Engineering, P.O. Box 16300, FI-00076, Espoo, Finland.

O. D. Onelli, G. Jacucci, Dr. S. Vignolini
Melville Laboratory for Polymer Synthesis, Department of Chemistry, University of Cambridge, Lensfield Road, CB2 1EW, Cambridge, United Kingdom
E-mail: sv319@cam.ac.uk

[+]These authors contributed equally to this work

Keywords: cellulose nanofibrils; nanocellulose; scattering; whiteness; anomalous diffusion;

The understanding of the interaction between light and complex, random structures is key for designing and tailoring the optical appearance and performance of many materials that surround us, ranging from everyday consumer products, such as those for personal care, paints and paper, to light diffusers used in LED-lamps and solar cells. Here, we demonstrate that light transport in membranes of pure cellulose nanofibrils (CNF) can be controlled to achieve bright whiteness in structures only a few microns thick. This is in contrast to other materials, such as paper, which require hundreds of microns to achieve a comparable appearance. The diffusion of light in the CNF membranes is shown to become anomalous by

tuning the porosity and morphological features. Considering also their strong mechanical properties and biocompatibility, we propose such white coatings as a new application for cellulose nanofibrils.

Whiteness is achieved when light is elastically scattered multiple times in random media.[1] In general terms, the higher the number and the strength of the scattering events, the brighter the material appears.[2] This simple principle explains why many commercially available white products, such as paints and sun creams, are typically formulated with high refractive index nanoparticles (e.g. TiO_2) as scattering enhancers.[3] The use of such promoters improves the scattering efficiency of the material, and therefore reduces the volume required to obtain fully opaque white coatings. However, the widespread use of TiO_2 particles as scattering enhancers, for example in food, cosmetics, and paper, has recently raised serious health and environmental concerns.[4,5] Therefore, there is a real need to improve scattering efficiency using more sustainable and biocompatible materials.[6,7]

In nature, scattering is optimized in biopolymeric structures by the intricate design of the morphology and the spatial arrangement of the scattering elements.[8–10] In particular, dense random networks of nanofibers, due to the intrinsic polydispersity and anisotropy of the scattering elements, allow efficient packing and represent a particularly convenient strategy to optimize brightness in thin coatings. Fibrillar nanomaterials, such as cellulose nanofibrils (CNF), are therefore promising candidates due to their inherent morphology, excellent mechanical performance, wide availability, renewability, and biocompatibility.[11–15]

However, paradoxically, research on the optical properties of CNF-based materials has focused on the optimization of their transparency.[16,17] Therefore, the possibilities of using CNF to construct an efficient scattering medium have not been explored, although recently

their potential for high-haze diffusive optical elements for optoelectronic applications has been recognized.[18]

Here, we demonstrate a scalable and versatile approach for light management in CNF membranes. By inducing appropriate porosity and tuning the size distribution of the CNF in the membranes, we are able to modify their nanostructure and easily produce membranes with completely different optical appearance: from thick, highly transparent membranes to thin, bright white ones. The produced membranes are mechanically stable as they retain the amorphous domains and hemicelluloses of natural cellulose fibers, in contrast to films based on cellulose nanocrystals which are significantly more brittle.[6] Finally, we observe that light transport in strongly scattering CNF membranes unexpectedly undergoes anomalous diffusive behavior.

Membranes with different scattering properties are obtained by fractionating a CNF dispersion with a wide distribution of fibril diameters via a sequential centrifugation procedure, as schematically illustrated in **Figure 1**a. The finest fibrils (i.e. smallest diameters) are first isolated from the original CNF dispersion by repeated centrifugation, collection of the supernatant, dilution, and homogenization. Subsequently, the same procedure is repeated at a lower centrifugal speed in order to isolate a dispersion of slightly thicker fibrils, which is referred to as “medium fibrils” in the rest of the text. Finally, the sediment is collected, diluted and homogenized. The fibrils in this last dispersion are referred to as “coarsest fibrils” in the following discussion. The presented sequential centrifugation process results in the three dispersions of fibrils, **Figure 1**b. For a fixed concentration, the turbidity of the dispersions correlates with the expected average fibril size. The distribution of the fibril diameters for the three dispersions are estimated by Atomic-Force Microscopy (AFM), see **Figure S1** and **Figure S2,** Supporting Information. By measuring the diameters of more than 500 fibrils of

each dispersion, we observe that their distributions follow, in first approximation, a log-normal statistics with a long tail, especially for the coarsest fibrils. The mean (and respective standard deviation) of the log-normal distributions of the fibril diameters in the three dispersions are 4.2 (2.7), 5.6 (3.2), and 19.5 (13.2) nm, going from the finest to the coarsest fibrils.

Porous membranes from the fractioned CNF dispersions are then prepared as described in an earlier work.[19] In summary, the dispersion is vacuum filtered into a wet gel cake, followed by solvent exchange from water to 2-propanol, and further to octane, after which the gel cake is slowly dried in ambient conditions. The thickness of the membranes was controlled by the volume of dispersion filtered. For qualitative comparison, photographs of the resulting porous membranes of equal thickness (~10 µm) prepared from the dispersions of the finest, medium, and coarsest fibrils are shown in **Figure 1**c,d,e (right-hand side of the photographs). The membranes prepared from the finest, medium, and coarsest fibrils are referred to as the “transparent”, “semi-transparent”, and “white” porous membranes, respectively. The solvent exchange step is crucial for the porosity, and the consequent whiteness. For comparison, dense CNF films prepared from an equal volume of the corresponding dispersions which have been dried directly from water without the solvent-exchange process are displayed in **Figure 1**c,d,e (left-hand side of the photographs). The thicknesses of the dense, water-dried films are approximately half of those of the porous, octane-dried membranes, while the masses and lateral dimensions of the samples are nearly the same, indicating that the density of the films dried from water is approximately double of the porous membranes dried from octane. The reason for the densification of the CNF films upon drying from water is the combination of the capillary pressure of the evaporating water and the disruption of the hydrogen bonding network at the intersections of fibrils by water,[20]

as also known from the Campbell effect in papermaking.[21] When the solvent is exchanged to octane, the hydrogen bonding network between the fibrils is no longer disrupted by the solvent and the fibrils can be considered physically crosslinked, thus allowing the microstructure to resist the capillary pressure without collapsing.[19,22,23]

The densities of the porous membranes were comparable and in the range (0.81 ± 0.16) kg m^{-3}. However, the porosity characterization by nitrogen physisorption revealed a different distribution of pore sizes. The transparent membranes show the highest specific surface area (190 ± 4) m^2 g^{-1} and smallest pores, followed by the semi-transparent membranes with a lower specific surface area (175 ± 6) m^2 g^{-1} and slightly larger pores, while the white membranes show the lowest specific surface area (122 ± 3) m^2 g^{-1} and the largest pores. The pore size distributions obtained by nitrogen physisorption are shown in **Figure S3**, Supporting Information, and those estimated by image analysis from cross-sectional SEM micrographs are shown in **Figure S4** and **Figure S5**, Supporting Information.

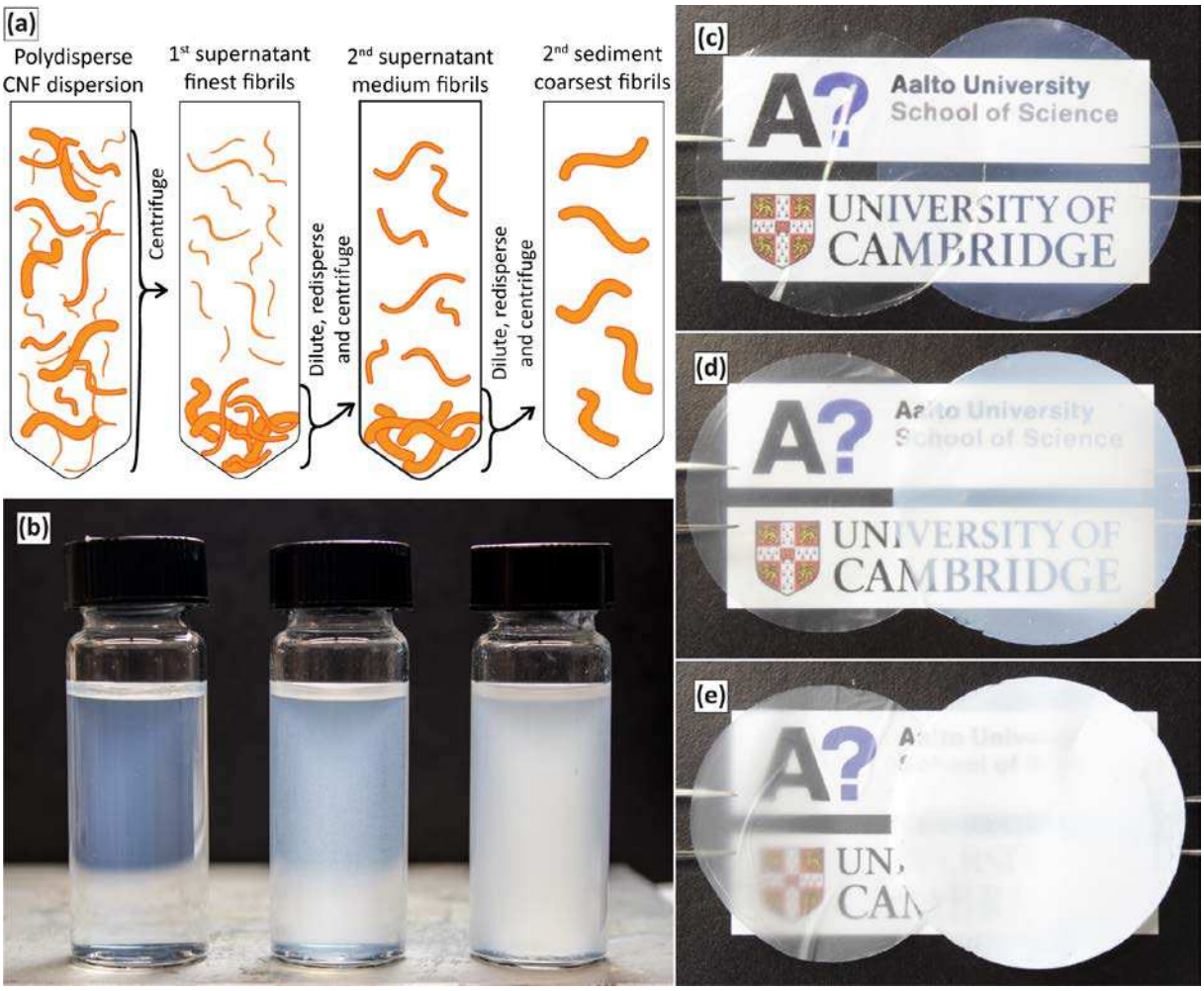

Figure 1. (a) Schematic illustration of the preparation procedure of the fractioned CNF dispersions by differential centrifugation. (b) Photograph of the resulting fractioned CNF dispersions after dilution to an equal concentration (0.9 g / L); left to right: finest, medium and coarsest fibrils. Photographs of the compact CNF films (left) and the ~10 µm thick, porous membranes of CNF dried from octane (right) when using (c) the finest, (d) the medium, and (e) the coarsest fibrils. The outer edges of the membranes and the compact films are approximately 1 cm off the paper underneath while the edge at the center of the image is in contact with the paper. In (c) the text remains fully legible underneath the transparent membrane made from the first supernatant, whereas in (e) the text cannot be resolved from under the white membrane fabricated from the coarsest fibrils. The semi-transparent membrane in (d) is the intermediate case. Masses of the compact CNF films and the corresponding porous membranes are 9.43 and 9.35 in (c), 9.53 and 9.11 in (d), and 8.34 and 7.95 mg in (e).

Total reflection spectra for the three types of membranes at a thickness of approximately 9 µm are reported in **Figure 2**a. Additional spectra for different thicknesses and a discussion of the wavelength dependence of the scattering properties are reported in

Figure S6, Supporting Information. It is important to notice, that the white membrane – which is only 9 µm thick - exhibits a high broadband reflectivity (60-80 %) for most of the visible range, reaching up to 90 % for the shorter wavelengths, with a wide-angular scattering distribution, see **Figure S7**. Supporting Information. In comparison, common filter paper reflects only ~50% of the incident light even though its thickness is 160 µm (**Figure S6**, Supporting Information). Thus, the white membranes can be considered to be between 20 to 30 times more efficient opacifiers than filter paper.

To fully characterize light transport in such systems, the total transmittance is measured as a function of the sample thickness: we fabricate different membranes and, for each type, the optical response is characterized in 5-6 samples. **Figure 2**b shows that the light transport in the transparent membrane can be described by diffusion approximation theory,[24] with a scattering mean free path of about 13.5 µm which is similar to that of paper (13 – 22 µm).[6,10] Surprisingly, the diffusion approximation, which generally describes the behavior of the majority of scattering materials, fails to describe the data obtained for the other two membranes. Therefore, to explain the experimental results we adopt an extended formalism, which describes light transport in super-diffusive and sub-diffusing systems,[25,26] where the total transmittance (T) scales with the sample thickness (L) as:[27]

$$T = \frac{1}{1+AL^{\alpha/2}} \qquad (1)$$

where A is a constant which depends on the scattering mean free path, the extrapolation length (a parameter that accounts for the internal reflections at the boundaries of the sample) and the absorption (the latter is negligible for cellulosic fibers),[25,26,28,29] and α is a parameter that describes the diffusion behavior, see Supporting Information. Notably when α = 2, the scaling behavior is equivalent to the one in the standard diffusion approximation.[24] As mentioned above, the data for the transparent samples is nicely fitted with α = 2, while those

for the two other membranes α is smaller than two. More specifically, we obtain α = 1.35 ± 0.10 and A = 0.14 ± 0.01 for the semi-transparent membrane, and α = 1.34 ± 0.15 and A = 0.65 ± 0.10 for the white one. Details of the fitting routines and the formula used for the fit are presented in the Supporting Information and in **Figure S8**, Supporting Information.

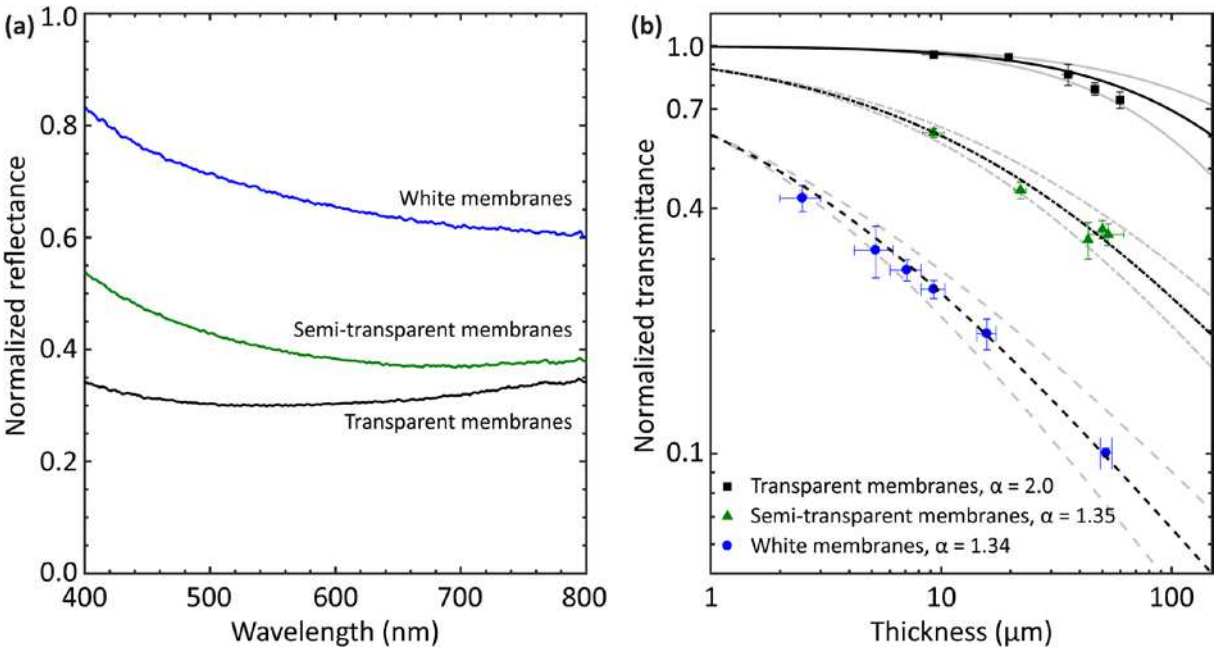

Figure 2. Optical characterization of the three types of membranes. (a) Total reflectance spectra at an approximate thickness of 9 µm. (b) Total transmittance at 500 nm as a function of sample thickness. The transmittance data series have been fitted according to Equation 1 by least-square regression (black lines). The transparent membranes (black squares) show a behavior very close to normal diffusion, α = (2.00±0.20) and A = (0.004±0.005). As the presence of inhomogeneity increases in the semi-transparent membranes (green triangles), the transmittance decays more steeply, α = (1.35±0.10) and A = (0.14±0.01). For the white films (blue circles), α = (1.34±0.15) and A = (0.65±0.10). The gray lines indicate the upper and lower bound for the value of the α parameter.

To further understand the anomalous diffusive behavior of the samples and the unusual scaling law, we analyze the morphology of the membranes by scanning electron microscopy (SEM) (**Figure 3**, and **Figure S4** and **Figure S5**, Supporting Information) and nitrogen physisorption (**Figure S3**, Supporting Information). The typical anisotropy (i.e. transversely isotropic in-plane orientation of fibrils) of CNF–based materials is observed for

all membranes when comparing the top-view SEM images (**Figure 3**a,b,c) and the cross-section exposed by either uniaxial tensile fracture (**Figure 3**a,b,c) or by cryo-microtoming in cyclohexane and freeze-drying (**Figure S4** and **Figure S7** Supporting Information).[22,30]

The SEM images reported in **Figure 3**a,d show that the transparent membranes are composed of a homogenous network of fine fibrils interspaced by small air voids. The pore size distribution clearly peaks around 30 nm (**Figure S3**, Supporting Information), whereas the average diameter of the fibrils is approximately 4 nm (see **Figure S2**a, Supporting Information). From the morphological analysis and scattering cross-section calculations (**Figure S10**, Supporting Information) we infer that the scattering in this case is mainly caused by the presence of the small air pores.

In contrast, in the case of the semi-transparent membranes (**Figure 3**b,e), we observe in the SEM images a certain number of significantly larger pores. This is confirmed by the broader distribution of pore sizes, extending up to 700 nm, as observed by nitrogen physisorption (**Figure S3**, Supporting Information) and image analysis of the cross-sectional SEM (**Figure S4** and **Figure S5**, Supporting Information).

Similarly, in the SEM images of white membranes (**Figure 3**c,f, **Figure S4**, and **Figure S9**, Supporting Information**)**, we recognize several anisotropic large pores (up to thousands of nanometers), as confirmed by the porosity characterization (**Figure S3** and **Figure S5,** Supporting Information). In this case, the main fraction of the volume is occupied by the network of fine fibrils interspaced by small pores. However, individual thicker fibrils (100-500 nm) are also sparsely embedded in this matrix in less dense regions.

We therefore speculate that the anomalous light transport for the semi-transparent and white membranes is induced by the combination of the anisotropy of the scatterers (i.e. in-plane orientation of fibrils and pores, see **Figure S4**, **Figure S5**, and **Figure S9** in Supporting

Information), and the rather wide distribution of sizes of both pores and fibrils, which consequently leads to a sparse spatial distribution of the stronger scatterers.

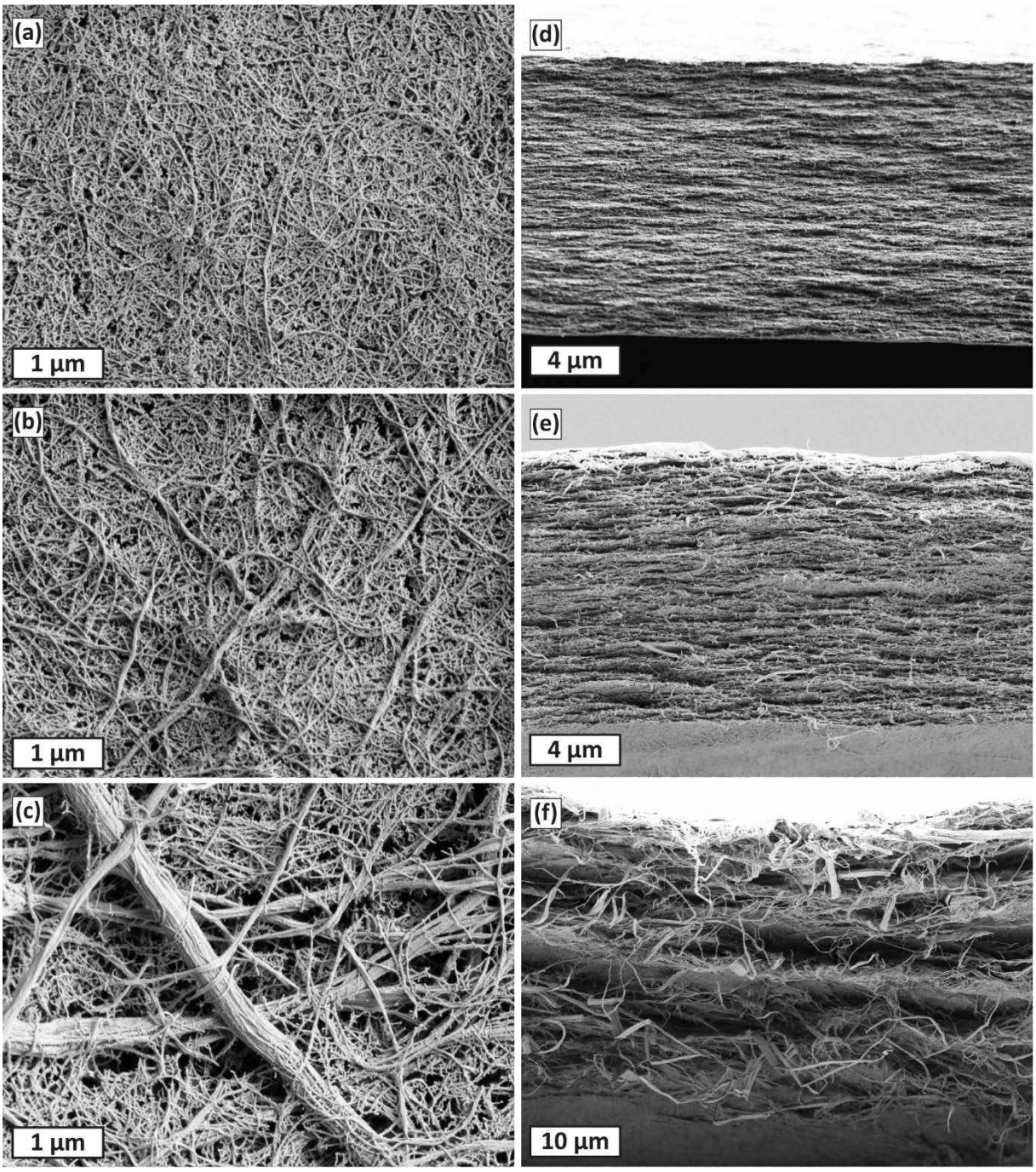

Figure 3. SEM micrographs of top surfaces of membranes (a-c) and their corresponding cross-sectional fracture surfaces (d-f). The micrographs show the transparent (a,d), semi-transparent (b,e), and white membranes (c,f). The layered structures observed in the cross-sectional fracture surfaces are likely to be caused by the fracture process and are not present

in the material prior to deformation,[20] as supported by the cross-sections exposed by cryo-microtoming and freeze-drying shown in **Figure S9**, Supporting Information.

To further demonstrate that the observed anomalous diffusion of light is not merely due to artifacts introduced in the sample preparation (e.g. due to the dependence of the morphological features on sample thickness), a speckle statistic experiment is performed.[31] The speckle patterns produced by the laser light transmitted through the investigated samples is imaged and recorded at more than 2000 separate locations (see Experimental section in Supporting Information and **Figure S12** and **Figure S13**). To better understand the data, we compare the response of white CNF membranes with standard filter paper (which is known to be a conventional diffuser with $\alpha = 2$ and scattering mean free path ≈ 18 μm at the wavelength used).[6]

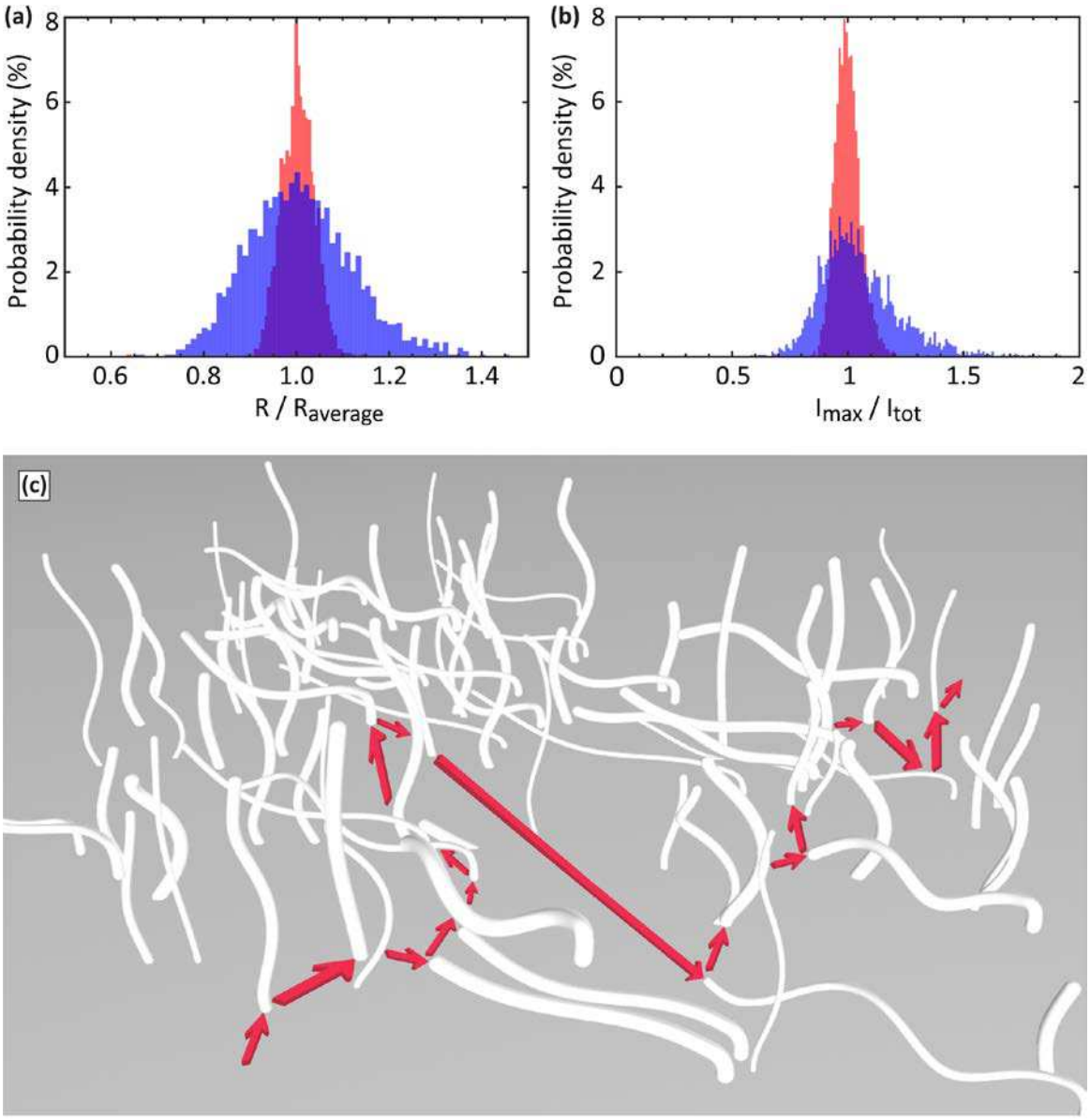

Figure 4. Statistical analysis of the speckle patterns for the white CNF membrane (blue, anomalous light diffusion) in comparison to standard filter paper (red, normal diffusion). (a) Distribution of the radii, R, of the speckle images normalized to their average $R_{average}$. (b) Distribution of the intensity, calculated as the ratio between the maximum intensity I_{max} and the total image intensity I_{tot}. For filter paper both histograms show a narrow distribution, as expected for a normally diffusive medium. In contrast, the population is considerably wider for the white CNF membranes, as expected for anomalous transport. (c) A scheme of a skewed random walk in which light (in red) is scattered more often in areas where the CNFs (in white) are more densely packed.

When light is transmitted through a standard diffusing sample, the individual speckle pattern varies between different sample locations but on average the radius (here measured by

the full width at half maximum of the intensity, FWHM) and intensity of the patterns are roughly constant as the light transport properties are the same across the specimen. In contrast, for an anomalously diffusive sample, the difference in speckle patterns between different sample locations is greater as the light paths can differ significantly depending on the local characteristics of the specimen, as shown in the literature.[27,31] As expected, the speckle statistics differ greatly for the white CNF membrane as compared to white filter paper (see **Figure 4**a,b). The high degree of spatial and intensity variability between the different speckle patterns from different locations on the sample further confirms the anomalous diffusive behavior of the CNF system. For the standard diffusive samples the radii and intensities of the speckle patterns are fairly constant at different positions, while for the white CNF membranes a broad distribution of values is observed (note that the radii and intensity have been normalized for better comparison). The speckle pattern intensities are inversely correlated with their radii as shown in **Figure S14**.

Therefore, we speculate that the observed anomalous diffusion response in white and semi-transparent CNF samples is due to three main factors: (i) the inhomogeneity in scattering strength due to the polydispersity of the fibrils (here we reasonably assume that each fibril can be considered a single scattering center); (ii) the inhomogeneity in the spatial distribution of fibrils, which could introduce longer steps between scattering events (**Figure S9**, Supporting Information); (iii) the anisotropy of the system due to in-plane orientation of the fibrils and anisotropic pores,[22,30] which implies that light propagation and scattering proceed differently when occurring across the plane or parallel to the plane of the membrane, see scheme in **Figure 4**c. We feel confident of excluding that the intrinsic birefringence of cellulose (i.e. refractive index of 1.539-1.596 along the fiber and 1.519-1.538 in the transverse direction) contributes strongly to this effect, as this would generate only negligible differences in the

scattering cross-section (see the calculations in **Figure S10** and the measured transmittance of s- and p-polarized light in **Figure S11**, both in Supporting Information).[32–34]

In conclusion, we report a cellulose-based system in which it is possible to manipulate light transport by simply tuning the morphology and the distribution of the CNF fibrils in porous membranes. A transition from standard to anomalous diffusion is observed in the disordered photonic nanostructures when larger anisotropy in the fibril distribution was introduced. Even though further optimization by fine-tuning of the porosity and of the diameters distribution the fibrils could lead to even thinner and brighter white membranes, we already obtain extremely high scattering efficiency in only few micron thickness,[6,9] and the white membranes can be considered between 20 to 30 times more efficient scatterers than white filter paper. We believe that our observation showcases the potential of using CNF and anomalous diffusion to produce next-generation efficient bright sustainable and biocompatible white materials.

Experimental Section

Experimental details can be found in the Supporting Information.

Supporting Information

Supporting Information is available from the Wiley Online Library or from the author.

All the research data supporting the publication are available from the University of Cambridge data repository (http://dx.doi.org/10.17863/CAM.XX).

Acknowledgements

M.S.T. and O.D.O contributed equally to this work. This work was supported by the BBSRC David Phillips fellowship [BB/K014617/1], the ERC-2014-STG H2020 639088, the Academy of Finland Centres of Excellence Programme (2014-2019), and the Academy of Finland project 264677. M.T. gratefully acknowledges the Emil Aaltonen Foundation, the Tiina and Antti Herlin Foundation and the Jenny and Antti Wihuri Foundation for their financial support. M.S.T. also gratefully acknowledges Prof. Thaddeus Maloney for supporting the nitrogen physisorption measurements, and Dr. Jani Seitsonen for his generous help with the preparation of cryo-microtomed microscopy samples. Aalto Nanomicroscopy Center is acknowledged for the use of the devices. O.D.O. acknowledges Mr. Connor Tann for advice on curve fitting and Dr. Villads E. Johansen for assistance and counsel on the speckle measurements. S.V. thanks Dr. Jacopo Bertolotti for invaluable discussion.

Received: ((will be filled in by the editorial staff))

Revised: ((will be filled in by the editorial staff))

Published online: ((will be filled in by the editorial staff))

References

[1] D. S. Wiersma, *Nat. Photonics* **2013**, *7*, 188.

[2] P. Vukusic, *Ophthalmic Physiol. Opt.* **2010**, *30*, 435.

[3] J. H. Braun, A. Baidins, R. E. Marganski, *Prog. Org. Coatings* **1992**, *20*, 105.

[4] A. Weir, P. Westerhoff, L. Fabricius, K. Hristovski, N. von Goetz, *Environ. Sci. Technol.* **2012**, *46*, 2242.

[5] S. Bettini, E. Boutet-Robinet, C. Cartier, C. Coméra, E. Gaultier, J. Dupuy, N. Naud, S. Taché, P. Grysan, S. Reguer, N. Thieriet, M. Réfrégiers, D. Thiaudière, J.-P. Cravedi,

M. Carrière, J.-N. Audinot, F. H. Pierre, L. Guzylack-Piriou, E. Houdeau, *Sci. Rep.* **2017**, *7*, 40373.

[6] S. Caixeiro, M. Peruzzo, O. D. Onelli, S. Vignolini, R. Sapienza, *ACS Appl. Mater. Interfaces* **2017**, *9*, 7885.

[7] J. Syurik, R. H. Siddique, A. Dollmann, G. Gomard, M. Schneider, M. Worgull, G. Wiegand, H. Hölscher, *Sci. Rep.* **2017**, *7*, 46637.

[8] P. Vukusic, B. Hallam, J. Noyes, *Science* **2007**, *315*, 348.

[9] S. M. Luke, B. T. Hallam, P. Vukusic, *Appl. Opt.* **2010**, *49*, 4246.

[10] M. Burresi, L. Cortese, L. Pattelli, M. Kolle, P. Vukusic, D. S. Wiersma, U. Steiner, S. Vignolini, *Sci. Rep.* **2014**, *4*, 6075.

[11] R. D. Perlack, L. L. Wright, A. F. Turhollow, R. L. Graham, B. J. Stokes, D. C. Erbach, *Biomass as Feedstock for A Bioenergy and Bioproducts Industry: The Technical Feasibility of a Billion-Ton Annual Supply*, **2005**.

[12] R. J. Moon, A. Martini, J. Nairn, J. Simonsen, J. Youngblood, *Chem. Soc. Rev.* **2011**, *40*, 3941.

[13] S. Tanpichai, F. Quero, M. Nogi, H. Yano, R. J. Young, T. Lindström, W. W. Sampson, S. J. Eichhorn, *Biomacromolecules* **2012**, *13*, 1340.

[14] T. Saito, R. Kuramae, J. Wohlert, L. A. Berglund, A. Isogai, **2013**, 6.

[15] N. Lin, A. Dufresne, *Eur. Polym. J.* **2014**, *59*, 302.

[16] M. Nogi, S. Iwamoto, A. N. Nakagaito, H. Yano, *Adv. Mater.* **2009**, *21*, 1595.

[17] M. S. Toivonen, S. Kurki-Suonio, F. H. Schacher, S. Hietala, O. J. Rojas, O. Ikkala, *Biomacromolecules* **2015**, *16*, 1062.

[18] H. Zhu, Z. Fang, C. Preston, Y. Li, L. Hu, *Energy Environ. Sci.* **2014**, *7*, 269.

[19] M. S. Toivonen, A. Kaskela, O. J. Rojas, E. I. Kauppinen, O. Ikkala, *Adv. Funct.*

Mater. **2015**, *25*, 6618.

[20] A. J. Benítez, J. Torres-Rendon, M. Poutanen, A. Walther, *Biomacromolecules* **2013**, *14*, 4497.

[21] A. Tejado, T. G. M. van de Ven, *Mater. Today* **2010**, *13*, 42.

[22] M. Henriksson, L. A. Berglund, P. Isaksson, T. Lindström, T. Nishino, *Biomacromolecules* **2008**, *9*, 1579.

[23] K. M. O. Håkansson, I. C. Henriksson, C. de la Peña Vázquez, V. Kuzmenko, K. Markstedt, P. Enoksson, P. Gatenholm, *Adv. Mater. Technol.* **2016**, *1*, 1600096.

[24] P. Sheng, *Introduction to Wave Scattering, Localization and Mesoscopic Phenomena*, Springer, Berlin, Germany, **2006**.

[25] A. Davis, A. Marshak, *Fractal Frontiers*, (Eds.: M. M. Novak, T. G. Dewey), World Scientific Publishing Co Pte Ltd, Singapore, **1997**.

[26] S. V Buldyrev, S. Havlin, A. Y. Kazakov, M. G. E. da Luz, E. P. Raposo, H. E. Stanley, G. M. Viswanathan, *Phys. Rev. E* **2001**, *64*, 41108.

[27] P. Barthelemy, J. Bertolotti, D. S. Wiersma, *Nature* **2008**, *453*, 495.

[28] D. Contini, F. Martelli, G. Zaccanti, *Appl. Opt.* **1997**, *36*, 4587.

[29] J. X. Zhu, D. J. Pine, D. A. Weitz, *Phys. Rev. A* **1991**, *44*, 3948.

[30] H. Sehaqui, N. Ezekiel Mushi, S. Morimune, M. Salajkova, T. Nishino, L. A. Berglund, *ACS Appl. Mater. Interfaces* **2012**, *4*, 1043.

[31] K. Vynck, J. Bertolotti, P. Barthelemy, D. Wiersma, in *Optical Properties of Photonic Structures, Interplay of Order and Disorder*, (Eds.: M. F. Limonov, R. M. De La Rue), London: CRC Press, Boca Raton, **2012**, pp. 227–248.

[32] H. Yano, J. Sugiyama, A. N. Nakagaito, M. Nogi, T. Matsuura, M. Hikita, K. Handa, *Adv. Mater.* **2005**, 17, 153.

[33] M. Nogi, H. Yano, *Adv. Mater.* **2008**, *20*, 1849.

[34] D. W. Van Krevelen, K. Te Nijenhuis, *Properties of Polymers*, Elsevier, Amsterdam, **2009**.